



Retaining Cornering Performance and Reducing Energy Consumption with Torque Vectoring and Suspensions Tuning

Michele Asperti^(✉), Michele Vignati, and Edoardo Sabbioni

Department of Mechanical Engineering, Politecnico di Milano, Via La Masa N.1,
20156 Milan, Italy
michele.asperti@polimi.it

Abstract. With the automotive industry's shift towards sustainability and energy efficiency, optimizing vehicle handling dynamics has become secondary. Additionally, there is a growing trend towards comfort-oriented design over handling performance. However, advancements such as integrating multiple independently controlled electric motors enable torque vectoring, offering a promising solution for reconciling these conflicting objectives. This paper proposes a novel approach to jointly improve vehicle handling and energy efficiency. Advanced simulation techniques are used to explore various suspension configurations to balance cornering performance and energy consumption. A torque vectoring controller is then designed in combination with meticulously tuned suspensions. This innovative approach, which considers active control design alongside suspension setup, achieves superior performance. Desired vehicle cornering capabilities are attained while ensuring significant efficiency in straight-line driving, which constitutes most road driving.

Keywords: Torque Vectoring · Vehicle Dynamics · Suspensions Setup Tuning · Vehicle Handling · Energy Efficiency

1 Introduction

Road vehicle users continue to demand sporty and high-performance vehicles, despite the automotive industry's current focus on achieving sustainable and energy-efficient solutions [1]. Consequently, in the context of suspensions, the industry's attention has shifted away from enhancing vehicle handling performance [2, 3]. Instead, suspension design now prioritizes ride comfort, with numerous approaches aimed at optimizing suspensions to improve overall ride quality [4, 5]. While car setup optimization [6] remains a fundamental aspect, recent advancements enabling the use of multiple electric motors in a single vehicle [7] have facilitated more advanced improvements. The implementation of In-Wheel Motors (IWMs) [8] allows for the easy deployment of Torque Vectoring (TV) systems, which control lateral dynamics by applying a yaw moment. Over the years, numerous TV controllers have been proposed [9, 10] to enhance vehicle lateral dynamics by actively tracking a yaw rate and/or sideslip angle reference. Conversely,

© The Author(s) 2024

G. Mastinu et al. (Eds.): AVEC 2024, LNME, pp. 525–532, 2024.

https://doi.org/10.1007/978-3-031-70392-8_75

some approaches utilize TV solely to improve overall vehicle efficiency [11]. A prevalent strategy lies between these two extremes, where TV controllers are designed to enhance lateral dynamics while allocating actuation torque to motors in a manner that minimizes power losses [12]. Additionally, TV controllers can adapt vehicle behavior to meet driver preferences by selecting a driving mode [13], allowing for on-demand modifications to the reference vehicle behavior, thus balancing vehicle handling and energy efficiency.

This paper investigates a novel approach to achieving optimal vehicle handling and high energy efficiency by jointly tuning vehicle suspensions and designing the torque vectoring control system. This integrated approach addresses the trade-off between vehicle cornering performance and energy efficiency by providing additional degrees of freedom. In particular, various configurations of combined suspension tuning and torque vectoring designs are evaluated in a simulation environment to assess their impact on cornering dynamics and energy efficiency.

2 Vehicle Model and Suspensions Tuning

The vehicle considered in this study belongs to the S-segment and is equipped with four independently controllable In-Wheel Motors (IWMs). The vehicle model for simulation purposes is developed using VI-CarRealTime software, incorporating five rigid bodies and 14 degrees of freedom. Specifically, the model used in this study is based on the validated SportCar model, originally representing an internal combustion engine vehicle, whose powertrain has been replaced with four In-Wheel Motors (IWMs).

Suspension angles, such as camber and toe, are typically set at neutral values in standard road cars to prevent excessive tire wear from scrubbing against the road. In contrast, these angles are often adjusted away from neutral in sports vehicles to enhance cornering response. Therefore, it is crucial to set these angles appropriately for the specific vehicle's purpose. In this study, two suspension setups are considered, as shown in Table 1. The baseline setup features suspension angles typical of road vehicles, ensuring proper drivability under all conditions. The sporty setup, instead, includes more aggressive suspension angles and a stiffened rear anti-roll bar to improve vehicle handling.

Table 1. Baseline and sporty vehicle suspensions setup details.

Parameter	Symbol	Baseline Setup	Sporty Setup
Front camber angle	γ_f	-0.5°	-4.5°
Front toe angle	τ_f	-0.05°	-0.15°
Rear camber angle	γ_r	-0.5°	-3.0°
Rear toe angle	τ_r	$+0.05^\circ$	$+0.15^\circ$
Front roll-bar stiffness	$k_{\theta,f}$	7040 Nm/rad	7040 Nm/rad
Rear roll-bar stiffness	$k_{\theta,r}$	21450 Nm/rad	42900 Nm/rad

3 Torque Vectoring Controller Design

The Torque Vectoring (TV) controller developed in this study is intended for implementation on a vehicle equipped with the baseline suspension setup, with the goal of replicating the cornering performance of the same vehicle when fitted with the sporty suspension setup. To achieve this goal, a reference generator for vehicle cornering has been designed. Specifically, the yaw rate has been chosen as the control variable, and the reference function incorporating exponential saturation, as outlined in [10], has been adopted in this study.

$$r_{ref} = \begin{cases} \frac{V}{l(1+K_{US}V^2)} \tau_{SW} \delta_{SW} = \alpha \delta_{SW} & \text{IF } \delta_{SW} \leq \delta_{SW}^* \\ r_{max} + (r^* - r_{max}) e^{\left(\frac{-\alpha(\delta_{SW} - \delta_{SW}^*)}{(r_{max} - r^*)} \right)} & \text{IF } \delta_{SW} > \delta_{SW}^* \end{cases} \quad (1)$$

In there, the maximum attainable yaw rate is the maximum achievable lateral acceleration normalized by the actual vehicle speed ($r_{max} = a_{y,max}/V$), r^* is the yaw rate value at which the transition between the linear and saturation regions occurs, $\delta_{SW}^* = r^*/\alpha$ is the steering wheel angle value at which this transition happens and τ_{SW} is the steering ratio between the steering wheel and the front wheels. Given the reference yaw rate function, its three main parameters (r_{max} , α , δ_{SW}^*) are obtained by fitting the reference to the yaw rate response of the sporty vehicle to steering pad constant speed maneuvers. These maneuvers have been performed at several different constant speeds by increasing the steering wheel angle at a rate of one degree per second until reaching the vehicle handling limits. The reference function characteristic coefficients are then regularized through a proper fitting over the achievable speed range for the vehicle for defining the yaw rate reference in each possible condition, with the results reported in Fig. 1.

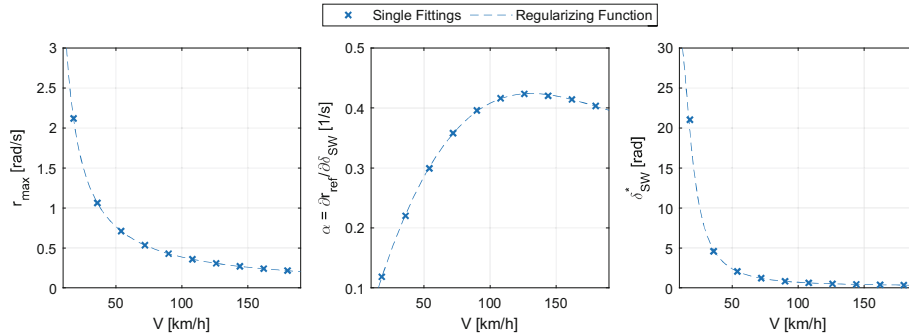


Fig. 1. Reference yaw rate function coefficients as function of vehicle speed.

The torque vectoring controller for tracking the desired yaw rate response defines the yaw moment to be deployed to the vehicle as the sum of a feedforward and a feedback contribution.

$$M_z = M_{z,FF} + M_{z,FB} = k_\delta \delta + k_P (r_{ref} - r) + k_I \int_0^t (r_{ref} - r) dt \quad (2)$$

The feedforward contribution is function of the wheel steering angle commanded by the driver, while the feedback contribution is the output of a PI controller aiming at minimizing the yaw rate deviation from its reference value. The feedforward gain (k_δ) is obtained by imposing that the static gain of the frequency response function relating the yaw rate response to the steering input is equivalent for the active and the sporty vehicle, resulting in the following

$$\mu_{\delta,ACTIVE}^r = \mu_{\delta,SPORTY}^r \rightarrow k_\delta = \frac{k_{y,f}k_{y,r}l}{k_{y,f}+k_{y,r}} \frac{\alpha_{SPORTY}-\alpha_{BASE}}{\alpha_{BASE}} \quad (3)$$

where $k_{y,f}$ and $k_{y,r}$ are the cornering stiffness of the front and rear axles respectively, l is the vehicle wheelbase and α_{BASE} and α_{SPORTY} are the slope of the linear yaw rate response region for the baseline and the sporty vehicles respectively. The feedback control gains (k_P, k_I) are instead tuned with a model-based approach with the objective of obtaining a robust and stable controlled system which performs as closely as possible to the sporty vehicle.

4 Results

The effectiveness of the proposed control strategy, implemented on a vehicle with the baseline suspension setup, in replicating the lateral dynamics performance of the vehicle with the sporty suspension setup, is evaluated through numerical simulations. The results encompass both transient and steady-state maneuvers, covering a range of scenarios from open-loop to closed-loop modalities, under high friction conditions ($\mu = 1.0$).

4.1 Straight Line Constant Speed Maneuver

A straight-line constant speed maneuver is simulated to evaluate the energy consumption effects of three different vehicle configurations. This maneuver was conducted at speeds ranging from 5 m/s to 50 m/s, in increments of 5 m/s. The simulation results are presented in Fig. 2 for the various running speeds. In there, the specific energy consumption (E_{sp}) increases more than linearly with vehicle speed due to aerodynamic resistance and

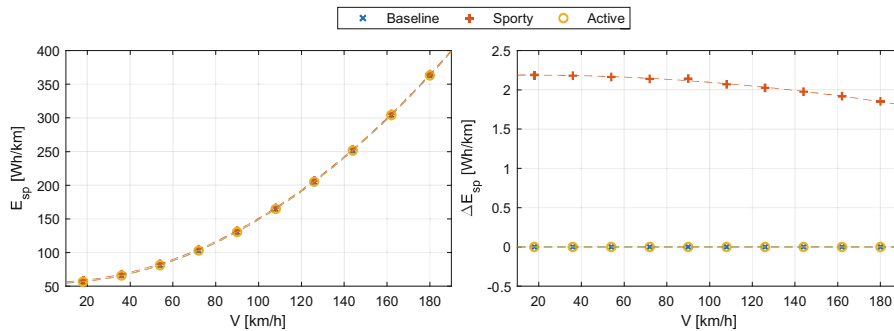


Fig. 2. Specific energy consumption and its variation with respect to the baseline vehicle for a straight-line constant speed maneuver across three vehicle configurations.

shows no significant differences among the three vehicle configurations. However, the variation in specific energy consumption (ΔE_{sp}) relative to the baseline vehicle indicates an increased energy demand for the sporty vehicle. This phenomenon may be attributed to the suspension angles, which causes tire scrubbing on the road, resulting in power losses due to lateral slip velocity at the tire-ground contact.

4.2 Constant Radius Cornering Maneuver

The steady-state handling performance of the proposed vehicle configurations under high friction conditions is evaluated using an ISO 4138 constant radius cornering maneuver. In this maneuver, the vehicle’s speed is progressively increased at a constant rate, and the steering wheel angle is adjusted in close-loop to maintain a circular trajectory. The speed is increased from 10 km/h until the baseline vehicle achieves at least 99% of the maximum attainable lateral acceleration for the selected turn radius. The cornering results for a specific maneuver with a 100 m turn radius are presented in Fig. 3. Additionally, Fig. 4 summarizes the handling and energy consumption performance across all the inspected turn radii.

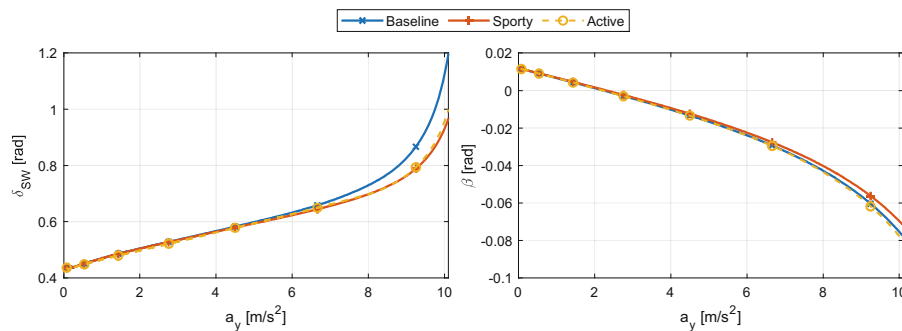


Fig. 3. Vehicle handling response during a constant radius cornering maneuver for a 100 m radius turn across three vehicle configurations.

The results in Fig. 3, illustrating the trend of the steering wheel angle as a function of vehicle lateral acceleration, indicate that the sporty and active vehicle configurations achieve almost equivalent cornering performance, both of which surpass that of the baseline configuration. Indeed, the baseline vehicle requires a greater steering wheel angle input to achieve the same turn radius. Additionally, both the baseline and active vehicle configurations exhibit similar sideslip angle responses, whereas the sporty vehicle is also capable of reducing the sideslip angle. The results in Fig. 4 indicate that the active vehicle configuration requires slightly more steering wheel angle input compared to the sporty configuration, while the baseline vehicle demands significantly more input than both. Furthermore, Fig. 4 demonstrates that both the sporty and active vehicle configurations consume less energy than the baseline configuration when executing a constant radius turn. Notably, the sporty vehicle achieves nearly five times the energy savings of the active vehicle. This significant reduction in energy consumption is primarily attributed to the lower longitudinal slip of the outer tires in the sporty vehicle, which

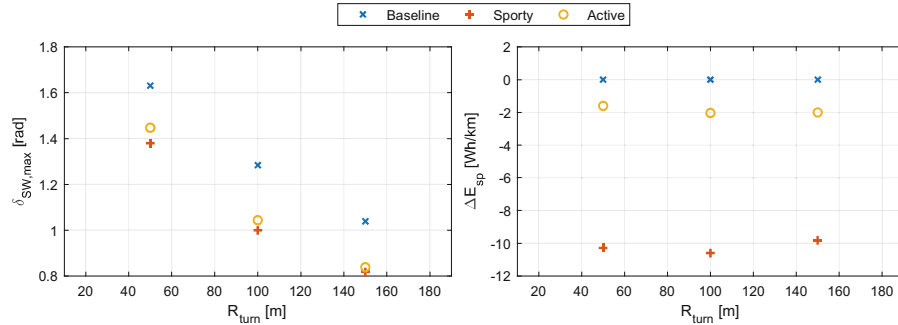


Fig. 4. Maximum steering wheel angle and specific energy consumption variation (ΔE_{sp}) with respect to the baseline vehicle during a constant radius cornering maneuver across three vehicle configurations.

is not employing increased longitudinal forces at outer wheels as the active vehicle is doing.

4.3 Double Lane Change Maneuver

The transient performance of the proposed vehicle configurations is evaluated using steering wheel closed-loop simulations based on an ISO 3888 double lane-change maneuver under high friction conditions. Figure 5 presents the results of this maneuver, comparing the performance of the three vehicle configurations.

An examination of the results in Fig. 5 reveals that the sporty and active vehicle configurations perform similarly under transient conditions, indicating an effective design and tuning of the torque vectoring controller. The trends observed in the steady-state tests are confirmed, showing that both the sporty and active vehicles generally enhance the cornering performance. Additionally, the active vehicle requires a slightly larger steering wheel angle input and exhibits a marginally higher sideslip angle compared to the sporty vehicle, which also confirms the steady-state results. In terms of power consumption, the baseline vehicle is the most demanding ($E_{sp,BASE} = 137.9$ Wh/km), followed by the active vehicle ($E_{sp,ACTIVE} = 132.4$ Wh/km), which consumes slightly more energy than the sporty vehicle ($E_{sp,SPORTY} = 130.8$ Wh/km).

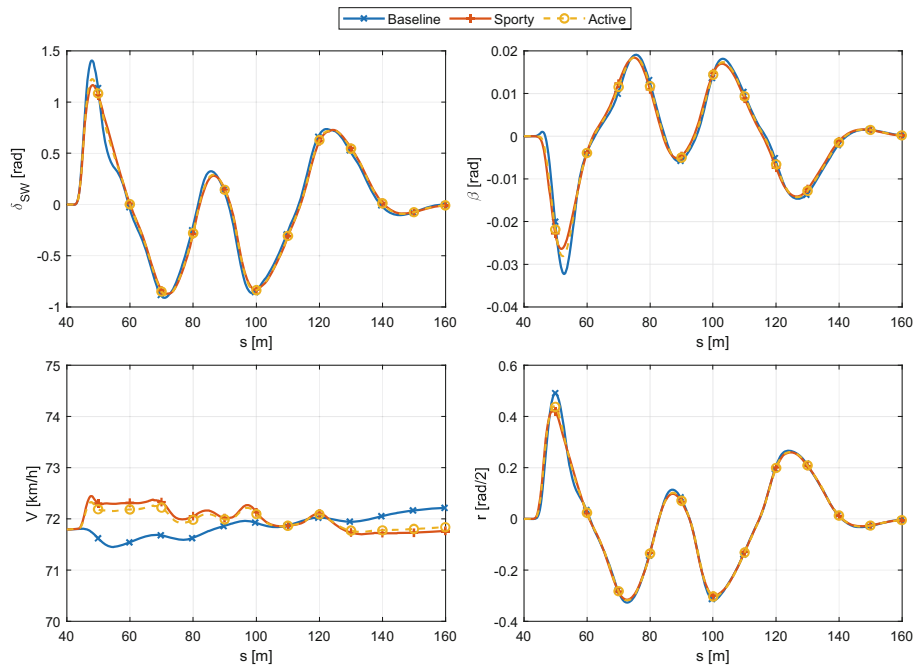


Fig. 5. Vehicle handling response during a double lane change maneuver in high friction conditions across three vehicle configurations.

5 Conclusions

The use of torque vectoring to enhance vehicle lateral dynamics has been extensively studied over the years. However, integrating a torque vectoring controller with suspension parameters tuning to improve cornering capabilities while ensuring good energy efficiency remains underexplored. In this study, baseline and sporty suspension setups have been defined and a torque vectoring controller designed for an active vehicle with the baseline suspension setup to emulate the handling characteristics of the sporty vehicle. Various steady-state and transient maneuvers have been simulated to demonstrate the method's effectiveness. Steady-state maneuver results confirm that the actively controlled vehicle can closely match the sporty vehicle performance by using torque vectoring to enhance the baseline vehicle handling. In terms of energy efficiency, the active vehicle outperforms the sporty vehicle in straight-line conditions but performs slightly worse in turns. Transient maneuver results corroborate the steady-state findings regarding handling, with the active vehicle's energy savings approaching those of the sporty vehicle.

References

1. Requia, W.J., Mohamed, M., Higgins, C.D., et al.: How clean are electric vehicles? evidence-based review of the effects of electric mobility on air pollutants, greenhouse gas emissions and human health. *Atmos. Environ.* **185**, 64–77 (2018)

2. Afkar, A., Mahmoodi-Kaleibar, M., Paykani, A.: Geometry optimization of double wish-bone suspension system via genetic algorithm for handling improvement. *Journal of Vibroengineering* **14**, 827–837 (2012)
3. Kwon, S.-J., Kim, T.-L., Kim, C.-J.: Optimal selection of suspension and tires for vehicles' cornering performance. *Machines* **10**, 1032 (2022)
4. Uys, P.E., Els, P.S., Thoresson, M.: Suspension settings for optimal ride comfort of off-road vehicles travelling on roads with different roughness and speeds. *J. Terramech.* **44**, 163–175 (2007)
5. Mitra, A.C., Soni, T., Kiranchand, G.R.: Optimization of automotive suspension system by design of experiments: a nonderivative method. *Adv. Acoust. Vibr.* **2016**, e3259026 (2016)
6. Wloch, K., Bentley, P.J.: Optimising the Performance of a Formula One Car Using a Genetic Algorithm. In: Yao, X., Burke, E.K., Lozano, J.A., et al. (eds.) *Parallel Problem Solving from Nature - PPSN VIII*, pp. 702–711. Springer, Berlin, Heidelberg (2004)
7. Rinderknecht, S., Meier, T.: Electric power train configurations and their transmission systems. *SPEEDAM* **2010**, 1564–1568 (2010)
8. Murata, S.: Innovation by in-wheel-motor drive unit. *Veh. Syst. Dyn.* **50**, 807–830 (2012)
9. Katsuyama, E., Yamakado, M., Abe, M.: A state-of-the-art review: toward a novel vehicle dynamics control concept taking the driveline of electric vehicles into account as promising control actuators. *Veh. Syst. Dyn.* **59**, 976–1025 (2021)
10. Asperti, M., Vignati, M., Sabbioni, E.: On torque vectoring control: review and comparison of state-of-the-art approaches. *Machines* **12**, 160 (2024)
11. De Filippis, G., Lenzo, B., Sorniotti, A., et al.: Energy-efficient torque-vectoring control of electric vehicles with multiple drivetrains. *IEEE Trans. Veh. Technol.* **67**, 4702–4715 (2018)
12. Pennycott, A., Novellis, L.D., Gruber, P., et al.: Enhancing the energy efficiency of fully electric vehicles via the minimization of motor power losses. In: *2013 IEEE International Conference on Systems, Man, and Cybernetics*, pp. 4167–4172 (2013)
13. Mangia, A., Lenzo, B., Sabbioni, E.: An integrated torque-vectoring control framework for electric vehicles featuring multiple handling and energy-efficiency modes selectable by the driver. *Meccanica* **56**, 991–1010 (2021)

Open Access This chapter is licensed under the terms of the Creative Commons Attribution 4.0 International License (<http://creativecommons.org/licenses/by/4.0/>), which permits use, sharing, adaptation, distribution and reproduction in any medium or format, as long as you give appropriate credit to the original author(s) and the source, provide a link to the Creative Commons license and indicate if changes were made.

The images or other third party material in this chapter are included in the chapter's Creative Commons license, unless indicated otherwise in a credit line to the material. If material is not included in the chapter's Creative Commons license and your intended use is not permitted by statutory regulation or exceeds the permitted use, you will need to obtain permission directly from the copyright holder.

